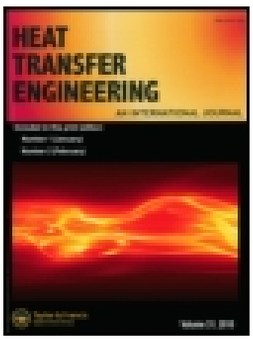

Heat Transfer Engineering

ISSN: 0145-7632 (Print) 1521-0537 (Online) Journal homepage: http://www.tandfonline.com/loi/uhte20

Volumetric Convective Heat Transfer Coefficient Model for Metal Foams

Hui Wang & Liejin Guo

To cite this article: Hui Wang & Liejin Guo (2018): Volumetric Convective Heat Transfer Coefficient Model for Metal Foams, Heat Transfer Engineering, DOI: 10.1080/01457632.2018.1432045

To link to this article: https://doi.org/10.1080/01457632.2018.1432045

Accepted author version posted online: 01 Feb 2018.

Volumetric Convective Heat Transfer Coefficient Model for Metal Foams

Hui Wang and Liejin Guo*

State Key Laboratory of Multiphase Flow in Power Engineering, Xi'an Jiaotong University

*Address correspondence to Professor Liejin Guo, State Key Laboratory of Multiphase Flow in Power Engineering, Xi'an Jiaotong University, Xi'an, 710049, China.

Email: lj-guo@xjtu.edu.cn

Phone Number: +86-29-82663895; Fax Number: +86-29-82669033

ABSTRACT

This study investigates the heat transfer in metal foams assuming that all the foam cells are cubic. An improved model for the volumetric convective heat transfer coefficient of metal foam was obtained by considering the convective heat transfer and the thermal conduction in the connected foam ligaments. Numerical simulations of a metal foam-filled channel were performed using the local thermal non-equilibrium model to evaluate the model. The theoretical and experimental data agree better with the present model than with other models. The velocity gradient near the metal foam-filled channel wall is greater than in an empty channel, with the

wall boundary layer becoming thinner. The temperature differences between the fluid and solid phases are predicted by the model with the pore density affecting the volumetric convective heat transfer coefficient more than the porosity. The volumetric convective heat transfer coefficient significantly increases as the pore density increases. However, the relationship between the volumetric convective heat transfer coefficient and the porosity is not linear. As the porosity increases, the volumetric convective heat transfer coefficient first increases and then decreases. The effect of the solid thermal conductivity on the volumetric convective heat transfer coefficient has an upper limit with a critical value of the solid thermal conductivity for the present conditions.

INTRODUCTION

In recent years, heat transfer in metal foams has gained significant attention due to its high heat transfer rates in thermal engineering applications, such as compact heat exchangers, heat pipes, electronic cooling systems and solar collectors [1-4].

Numerous studies have investigated the heat transfer characteristics in metal foams [5-10]. Han et al. [4] made a review of metal foam and metal matrix composites for heat exchangers and heat sinks. The result showed that metall foams seem to have a particularly bright future in heat sink applications. Calmidi [5] investigated the thermal transport in metal foams with measurements of the outer wall temperatures and inlet and outlet fluid temperatures. The wall

heat transfer coefficient of a metal foam-filled channel was calculated from the measured data. Boomsma et al. [2] conducted similar measurements using the wall heat transfer coefficient to evaluate the performance of a metal foam compact heat exchanger. Noh et al. [11] examined the heat transfer coefficient for a constant heat wall flux, obtaining significant enhancement of the wall Nusselt number compared with laminar flow in an empty annulus. Kim et al. [6] showed that the wall Nusselt number was significantly higher for low permeability aluminum foams and gave a correlation for predicting the wall Nusselt number of a metal foam-filled channel. Tzeng [12] examined the local and average wall Nusselt numbers, finding that a conductive pipe in an aluminum foam heat sink gave effective spatial thermal regulation. Zhao et al. [13] analyzed the forced convective heat transfer characteristics in high porosity open-cell metal foam-filled tube heat exchangers, finding that the wall heat transfer coefficient on the metal foam-filled tube was approximately three times higher than that on a longitudinally-finned tube. Jeng and Tzeng[14] numerically investigated the fluid flow and heat transfer characteristics of a metallic foam heat sink under a laminar slot jet confined by a parallel wall. Huang et al. [15] found that convective heat transfer was considerably enhanced by porous medium inserts in a tube. Yang et al. [16] investigated the effectiveness of porous material inserts within a tube and found that for low pumping powers, the wall Nusselt number of a tube with a porous medium core was higher than that of a tube with a porous medium layer covered the wall.

These studies all focused on the wall heat transfer coefficient. References [17, 18] note that the enhanced surface area between the solid and fluid phases is the main reason for metal foams enhancing the wall heat transfer coefficient. Therefore, a better understanding of the volumetric convective heat transfer coefficient will enhance understanding of the metal foam heat transfer mechanism. However, only a few studies have investigated the volumetric convective heat transfer coefficient because the solid and fluid temperatures inside the metal foam are difficult to measure [19]. Golombok et al. [20] used a non-steady-state method to experimentally measure the volumetric convective heat transfer coefficient between hot air and metal fibers. They found that the volumetric convective heat transfer coefficient rapidly increased as the gas flow rate increased. Younis and Viskanta [21] investigated the effect of pore diameter on the volumetric convective heat transfer coefficient by testing two different types of ceramic foams with smaller pore diameters giving higher volumetric convective heat transfer coefficients. Hwang et al. [22] experimentally measured the volumetric convective heat transfer coefficient in aluminum foams and developed empirical correlations for the pore Nusselt number in terms of the pore Reynolds number for various foam porosities. Giani et al. [23] measured the volumetric convective heat transfer coefficients in FeCrAlY and Cu foams having different pore sizes. The derived correlation was similar to findings of previous studies on the heat transfer in tube bundles [9]. Jiang et al. [24] presented two different methods to obtain volumetric convective heat transfer coefficients in sintered bronze porous media by a lumped capacitance method and a

one-dimensional numerical analysis method. The results of the two methods agreed but the lumped capacitance method was much simpler.

Two models used to model the convective heat transfer process in metal foams are the local thermal equilibrium and local thermal non-equilibrium methods. The local thermal equilibrium model assumes that the solid phase temperature is equal to the fluid phase temperature and only involves one energy equation. Theoretical and numerical analyses with this model are quite easy. However, the local thermal equilibrium assumption is inadequate when the temperature difference between the solid and fluid phases is too large. Therefore, the local thermal non-equilibrium model is used for large temperature differences. The key parameter in the non-equilibrium model is the volumetric convective heat transfer coefficient between the solid and fluid phases, h_{sf}. Lu et al. [25] developed a cubic cell model to describe a foam network of connected struts. The fluid temperature was obtained from this model but the volumetric convective heat transfer coefficient was not analyzed. Most studies using the non-equilibrium model still use the volumetric convective heat transfer coefficient correlation presented for staggered tube bundles in crossflow which does not consider the interactions between the metal foam ligaments.

This study models the metal foam volumetric convective heat transfer coefficient by considering the convective heat transfer in the pores and the thermal conduction in the connected foam ligaments. Results of a numerical study of a metal foam-filled channel are then compared

to the experimental and numerical results obtained by Zhao et al. [26]. The velocity distribution and the fluid and solid temperature distributions in the metal foam-filled channel are investigated. The results show the effects of the metal foam parameters (i.e., porosity, pore density and solid thermal conductivity) on the volumetric convective heat transfer coefficient.

DERIVATION OF THE VOLUMETRIC CONVECTIVE HEAT TRANSFER COEFFICIENT

Figure 1 shows the complex structure of a typical metal foam. The foam has a three-dimensional open-cell structure with interconnected cells. Metal foams have two characteristic parameters, the porosity, ε, and the pore density, PPI (pores per inch). The porosity is defined as the ratio of the void volume to the total volume. The pore density refers to the pore size, which is determined by counting the number of pores per inch. As the actual structure of metal foam is too complex for theoretical analyses, the structure has usually been approximated by polyhedrons [27-29]. Figure 2 shows the cubic model, which is a simple approximation [5, 25].

The cubic model includes several perpendicular equivalent cylinders. The diameter of each cylinder is d_f; the length of each cylinder is d_p; and the space between two adjacent cylinders is also d_p. The forced convective flow across the metal foam can be assumed to be analogous to the flow across a bank of connected cylinders.

Figure 2 shows that the cubic model has a repeated geometrical structure. Figure 3 shows the repeatable elements of the metal foam. The local cell is used as the analysis object. The local cell includes six cylinders, marked l_{1c}, l_{2c}, l_{3c}, l_{4c}, l_{5c} and l_{6c}. The length of each cylinder is $0.5d_p$ and the diameter of each cylinder is d_f. The temperatures at the tip of each cylinder are T_1, T_2, T_3, T_4, T_5 and T_6. The cylinders meet at the center point *C*, which is the coordinate system origin. The temperature at the center point is T_C. The volumetric convective heat transfer coefficient between the foam ligaments and the fluid is obtained by analyzing the convective heat transfer around the cylinders and the thermal conduction in the cylinders.

The present study assumes that the metal foam temperatures are at steady state. The radiation heat transfer within the metal foam is neglected because the radiation heat transfer is usually at least one order of magnitude smaller than the forced convection heat transfer in typical structures[9]. Therefore, the foam ligaments only exchange heat with the fluid. The heat conduction equation along the cylinder, l_{1c}, is:

$$\frac{d^2T_{1c}}{dx^2}+\frac{\Phi}{k_s}=0 \tag{1}$$

T_{1c} is the temperature of cylinder $l_{1c,}$ k_s is the thermal conductivity of the metal foam and Φ is the heat transfer source defined as:

$$\Phi=-\frac{Q_1}{V_1}=-\frac{4Q_1}{\pi d_f^2 d_p} \tag{2}$$

V_l is the volume of cylinder and Q_1 is the convective heat transfer rate between cylinder l_{1c} and the air. Per Newton's Law of Cooling, Q_1 is:

$$Q_1 = A_h h(T_{1c} - T_f) = \frac{1}{2}\pi d_f d_p h(T_{1c} - T_f) \tag{3}$$

A_h is the heat transfer area for cylinder l_{1c} and h is the convective heat transfer coefficient which can be estimated from correlations for staggered tube banks in crossflow [30]:

$$h = \begin{cases} 0.76\dfrac{k_f}{d_f} Re_d^{0.4} Pr^{0.37} (1 \le Re_d \le 40) \\ 0.52\dfrac{k_f}{d_f} Re_d^{0.5} Pr^{0.37} (40 \le Re_d \le 1000) \\ 0.26\dfrac{k_f}{d_f} Re_d^{0.6} Pr^{0.37} (1000 \le Re_d \le 2\times 10^5) \end{cases} \tag{4}$$

The Reynolds number is defined as $Re_d = \rho u d_f / \varepsilon\mu$.

Substituting Eqs. (2) and (3) into Eq. (1) gives:

$$\frac{d^2 T_{1c}}{dx^2} - \frac{2h}{k_s d_f}(T_{1c} - T_f) = 0 \tag{5}$$

Let

$$\theta = T_{1c} - T_f \tag{6}$$

and

$$m = \sqrt{\frac{2h}{k_s d_f}} \tag{7}$$

Therefore, Eq. (5) can be rewritten as:

$$\frac{d^2\theta}{dx^2} - m^2\theta = 0 \tag{8}$$

Equation (8) is a second-order, linear, homogeneous differential equation. The general solution is:

$$\theta = C_1 e^{mx} + C_2 e^{-mx} \tag{9}$$

The boundary conditions for cylinder l_{1c} are:

$$x = -0.5d_p, \quad \theta = T_1 - T_f \tag{10}$$

$$x = 0, \quad \theta = T_c - T_f \tag{11}$$

Therefore, the temperature of cylinder l_{1c} is:

$$T_{1c} = T_f + \frac{(-T_1 + T_f)\sinh(mx) + (T_c - T_f)\sinh[m(0.5d_p + x)]}{\sinh(0.5md_p)} \tag{12}$$

The heat flux at point 1 entering cylinder l_{1c} can be obtained using Fourier's Law of Heat Conduction:

$$q_{1i} = -k_s A_{cs} \frac{dT_{1c}}{dx}\Big|_{x=-0.5d_p} = mk_s \frac{\pi d_f^2}{4} \frac{(T_1 - T_f)\cosh(-0.5md_p) - (T_c - T_f)}{\sinh(0.5md_p)} \tag{13}$$

Similarly, the heat flux at point C on cylinder l_{1c} is:

$$q_{1o} = -k_s A_{cs} \frac{dT_{1c}}{dx}\Big|_{x=0} = mk_s \frac{\pi d_f^2}{4} \frac{(T_1 - T_f) - (T_c - T_f)\cosh(0.5md_p)}{\sinh(0.5md_p)} \tag{14}$$

Using energy conservation, the convective heat transfer rate between cylinder l_{1c} and the air should be equal to the heat flux difference between q_{1i} and q_{1o}:

$$Q_1 = q_{1i} - q_{1o} = mk_s \frac{\pi d_f^2}{4} \frac{(T_1 + T_c - 2T_f)\left[\cosh\left(0.5md_p\right) - 1\right]}{\sinh(0.5md_p)} \tag{15}$$

Similarly, the convective heat transfer rates for the other five cylinders can also be obtained as:

$$Q_2 = q_{2i} - q_{2o} = mk_s \frac{\pi d_f^2}{4} \frac{(T_2 + T_c - 2T_f)\left[\cosh\left(0.5md_p\right) - 1\right]}{\sinh(0.5md_p)} \tag{16}$$

$$Q_3 = q_{3i} - q_{3o} = mk_s \frac{\pi d_f^2}{4} \frac{(T_3 + T_c - 2T_f)\left[\cosh\left(0.5md_p\right) - 1\right]}{\sinh(0.5md_p)} \tag{17}$$

$$Q_4 = q_{4i} - q_{4o} = mk_s \frac{\pi d_f^2}{4} \frac{(T_4 + T_c - 2T_f)\left[\cosh\left(0.5md_p\right) - 1\right]}{\sinh(0.5md_p)} \tag{18}$$

$$Q_5 = q_{5i} - q_{5o} = mk_s \frac{\pi d_f^2}{4} \frac{(T_5 + T_c - 2T_f)\left[\cosh\left(0.5md_p\right) - 1\right]}{\sinh(0.5md_p)} \tag{19}$$

$$Q_6 = q_{6i} - q_{6o} = mk_s \frac{\pi d_f^2}{4} \frac{(T_6 + T_c - 2T_f)\left[\cosh\left(0.5md_p\right) - 1\right]}{\sinh(0.5md_p)} \tag{20}$$

The total convective heat transfer rate of the local cell is the sum of the heat transfer rates of the six cylinders:

$$Q_h = \sum_{i=1}^{6} Q_i = h_{sf} a_{s_f} V_c (\overline{T_s} - T_f) \tag{21}$$

h_{sf} is the volumetric convective heat transfer coefficient, V_c is local cell volume and a_{sf} is the surface area density which can be calculated from:

$$a_{sf} = \frac{6A_h}{V_c} = \frac{3\pi d_f}{(d_p)^2} \tag{22}$$

In most thermal applications with air and water as the working fluids, the convective heat transfer coefficient, h, ranges from 10^2 to 10^4 W/(m^2·K), the diameter of the metal foam, d_f, is on the order of 10^{-4} m and the thermal conductivity of the metal foam, k_s, is on the order of 10^2 W/(m·K), which results in a small Biot number, $Bi = hd_f/k_s \ll 1$. Therefore, the average temperature of each cylinder can be estimated as the mean of the temperatures at the two ends:

$$\overline{T_{iC}} = T_C + T_i \left(i = 1, 2 \cdots 6\right) \tag{23}$$

Given that each cylinder has the same shape and volume, the average temperatures of the six cylinders in the local cell, $\overline{T_s}$, are:

$$\overline{T_s} = \sum_{i=1}^{6} T_{iC} = \left(\sum_{i=1}^{6} T_i + 6T_c\right) \Big/ 12 \tag{24}$$

Combining Eqs. (21), (22) and (24) gives the volumetric convective heat transfer coefficient as:

$$h_{sf} = \frac{mk_s d_f}{d_p} \tanh(0.5md_p) \tag{25}$$

MODEL EVALUATION

Physical Model

The present volumetric convective heat transfer coefficient model was evaluated using numerical simulations of a metal foam-filled channel. The numerical results from the present model were compared to the experimental results and the numerical results obtained by Zhao et al. [26] using the Zukauskas model.

Figure 4 shows the physical model of the metal foam-filled channel and the cylindrical coordinate system. The length and height of the channel were 0.127 and 0.012 m, respectively, which were the same measurements as in the experimental setup of Zhao et al. [26]. Tests 4 and 10 in Zhao et al. [26] were used for the comparisons. Table 1 lists the structural parameters of the foam samples. The porosities of the two samples were established as follows. For sample 10, as described in Zhao et al. [26], the foam ligaments were solid, without any inner holes. Therefore, the porosity of sample 10 was calculated as:

$$\rho_r = 1 - \varepsilon \tag{26}$$

where ρ_r is the relative density. The porosity of sample 10 was 0.918.

However, as mentioned in their study, the ligaments of sample 4 were hollow. Therefore, the relationship between the porosity, ε, and relative density, ρ_r, was more complex:

$$\rho_r = (1 - \varepsilon)(1 - r^2) \tag{27}$$

r is the inner-to-outer diameter ratio. The porosity of sample 4 was 0.88.

Mathematical Formulations

The simulations assumed that the flow was incompressible and steady. The metal foam was treated as a homogeneous, isotropic porous media. The radiation heat transfer was neglected because the lowest temperature was below 100 °C. Based on these assumptions, the governing equations for this problem are as follows:

Continuity equation:

$$\nabla \cdot (\vec{v}) = 0 \tag{28}$$

The Darcy-Brinkman-Forchheimer momentum model for porous media [31, 32] was used to describe the fluid transport in the metal foam.

$$\frac{1}{\varepsilon^2}(\vec{v} \cdot \nabla)\vec{v} = -\frac{\nabla p}{\rho_f} + \frac{\mu_f}{\rho_f \varepsilon}\nabla^2(\vec{v}) - (\frac{\mu_f}{\rho_f K}\vec{v} + \frac{F}{\sqrt{K}}|\vec{v}|\vec{v}) \tag{29}$$

ρ_f is the fluid density, μ_f is the dynamic viscosity of the fluid, K is the permeability of the metal foam and F is the inertial coefficient. The permeability, K, and inertial coefficient, F, determine the pressure gradient in the metal foam and are strongly dependent on the metal foam structure. They can be estimated from the correlations presented by Calmidi [5]:

$$K = 0.00073(1-\varepsilon)^{-0.224}\left(\frac{d_f}{d_p}\right)^{-1.11} d_p^2 \tag{29}$$

$$F = 0.00212(1-\varepsilon)^{-0.132}\left(\frac{d_f}{d_p}\right)^{-1.63} \tag{30}$$

Where d_f is the fiber diameter of the metal foam and d_p is the cell size.

The local thermal non-equilibrium model, which describes heat transport between the foam ligaments and the fluid, was used to evaluate the volumetric heat transfer coefficient. This model has energy equations for the fluid and solid phases with each containing terms for the heat transfer between the solid and fluid phases.

Energy equation for the solid phase:

$$\nabla \cdot \left[k_{se} \nabla T_s\right] + h_{sf} a_{sf} \left(T_f - T_s\right) = 0 \tag{31}$$

Energy equation for the fluid phase:

$$\rho_f c_f (\vec{v}) \cdot \nabla T_f = \nabla \cdot \left[\left(k_{fe} + k_d\right) \nabla T_f\right] + h_{sf} a_{sf} (T_s - T_f) \tag{33}$$

Here, h_{sf} in Eqs. (31) and **Error! Reference source not found.** was determined by the model discussed in Eq. (25), ρ_f is the fluid density, ρ_s is the solid density, T_s is the solid temperature, T_f is the fluid temperature and k_d is thermal conductivity due to the thermal dispersion that results from the influence of the fluid tortuosity in the metal foam:

$$k_d = 0.1 \rho u C_f \sqrt{K} \tag{32}$$

k_{se} is the effective solid conductivity and k_{fe} is the effective fluid conductivity calculated using the method presented by Boomsma and Poulikakos [33]:

$$k_{eff} = \frac{\sqrt{2}}{2(R_A + R_B + R_C + R_D)} \tag{33}$$

$$R_A = \frac{4\lambda}{(2e^2 + \pi\lambda(1-e))k_s + (4 - 2e^2 - \pi\lambda(1-e))k_f} \tag{34}$$

$$R_B = \frac{(e-2\lambda)^2}{(e-2\lambda)e^2 k_s + (2e-4\lambda-(e-2\lambda)e^2)k_f} \tag{35}$$

$$R_C = \frac{(\sqrt{2}-2e)^2}{2\pi\lambda^2(1-2e\sqrt{2})k_s + 2(\sqrt{2}-2e-\pi\lambda^2(1-2e\sqrt{2})k_f} \tag{36}$$

$$R_D = \frac{2e}{e^2 k_s + (4-e^2)k_f} \tag{37}$$

With

$$\lambda = \sqrt{\frac{\sqrt{2}(2-(5/8)e^3\sqrt{2}-2\varepsilon)}{\pi(3-4e\sqrt{2}-e)}},\ e = 0.339 \tag{38}$$

The effective solid conductivity, k_{se}, could be obtained by setting k_f=0. Similarly, the effective fluid conductivity, k_{fe}, could be obtained by setting k_s=0.

Boundary Conditions

In Zhao et al. [26], the upper-wall of the channel was adiabatic while the lower-wall was uniformly heated. The heat flux at the lower-wall was directly applied to the channel. Then, the heat flux was transferred to the solid and fluid phases by conduction and convection. As discussed earlier [34-36], there were two approaches to address heat flux bifurcation for the given boundary conditions. One approach assumes that the total heat flux, q_w, is divided between the two phases per their effective thermal conductivities and the corresponding temperature gradients. The other approach assumes that each individual phase at the wall receives an equal amount of the total heat flux, q_w. The first approach was used in the present study. The boundary conditions were specified as follows:

$$T_f = T_{in},\ \frac{\partial T_s}{\partial x} = 0 \qquad at\ x = 0 \qquad (39)$$

$$\frac{\partial T_f}{\partial x} = 0,\ \frac{\partial T_s}{\partial x} = 0 \qquad at\ x = L \qquad (40)$$

$$q = q_w = k_{fe}\frac{\partial T_f}{\partial y} + k_{se}\frac{\partial T_s}{\partial y},\ T_s = T_f \qquad at\ y = 0 \qquad (41)$$

$$q = 0 \qquad at\ y = H \qquad (42)$$

Numerical Method

The commercial computational fluid dynamics software FLUENT 14.5 was used for the simulations. The phase-coupled SIMPLE algorithm was used for the pressure and velocity coupling. The second-order upwind scheme was used to discretize the governing equations. A convergence criterion of 10^{-10} was prescribed for the velocity and temperature fields. The grid independence study showed that a uniform mesh with 127×46 control volumes produced grid-independent solutions. All the subsequent flow and heat transfer computations used this mesh density.

Data Reduction

The average Nusselt number of the channel wall is defined as:

$$Nu = \frac{1}{L}\int_0^L Nu(x)dx \qquad (43)$$

L is the channel length and $Nu(x)$ is the local Nusselt number:

$$Nu(x) = \frac{q_w}{T_w(x) - T_{in}}\frac{D_h}{k_f} \qquad (44)$$

q_w is the heat flux at the wall, T_{in} is the fluid temperature at the channel inlet, $T_w(x)$ is the local wall temperature, k_f is the thermal conductivity of the fluid phase and D_h is hydraulic diameter of the channel:

$$D_h = 2WH/(H+W) \tag{45}$$

H is the channel height and W is the channel width.

Model Validation

The numerical predictions of the present model were compared with the numerical and experimental results of Zhao et al. [26] to obtain the average Nusselt number. The numerical results of Zhao et al. [26] were obtained using the volumetric heat transfer coefficient model presented by Zukauskas [30] while the numerical results of the present study were obtained using the model given as Eq. (25).

Figure 5 compares the average Nusselt numbers for sample 4. Here, the simulations using the present volumetric convective heat transfer coefficient model correspond well with the experimental data. The differences between the experimental data and the simulation results for the present model are smaller than the differences for Zhao et al. [26], especially at higher Reynolds numbers.

Figure 6 compares average Nusselt numbers for sample 10. The simulation results agree well with the experimental data. The predicted results with the Zukauskas model are much higher than the experimental data while the present results are closer to the experimental data.

The differences between the current simulations and those of Zhao et al. [26] show that the correlation developed by Zukauskas [30] does not account for the thermal conduction between the foam ligaments. The volumetric convective heat transfer coefficient in the simulations of Zhao et al. [26] do not consider the metal foam geometry. Unlike the Zukauskas model, the current model is based on the local cubic cell of the metal foam structure, the convective heat transfer in the cell and the thermal conduction between the foam ligaments. Figures 5 and 6 show the improved accuracy for the volumetric convective heat transfer coefficient with the present model.

Velocity Distribution

Figure 7 compares the velocity distributions in metal foam-filled and empty channels. The velocity distribution in the metal foam-filled channel is more uniform than in the empty channel. The velocity gradient near the wall in the metal foam-filled channel is the greater than that in the empty channel, with a thinner wall boundary layer. This occurs because flow mixing is enhanced in the metal foam-filled channel due to the irregular structure of the metal foam.

Fluid and Solid Temperature Distributions

Figure 8 shows the solid and fluid temperature distributions along the vertical direction at the cross-section of x/H=5. Figure 8(a) shows that the difference between the solid and fluid temperatures is small for sample 4. The solid temperature is slightly higher than the fluid temperature. Here, the temperature difference decreases as the dimensionless value, y/H,

increases. At the upper wall (y/H=1), the solid and fluid temperatures are almost the same. Unlike in sample 4, the temperature difference between the solid and fluid phases is quite large in sample 10, especially for the smaller Reynolds number of 2000.

Figure 9 shows the average solid and fluid temperatures over the cross-section of the channel along the flow direction. The average temperatures were calculated as:

$$T_m(x) = \frac{1}{u_m(x)H}\int_0^H uTdy \tag{46}$$

$u_m(x)$ is the average fluid velocity at the same cross-section defined by:

$$u_m(x) = \frac{1}{H}\int_0^H udy \tag{47}$$

Figure 9 (a) and (b) show that the average solid and fluid temperatures for samples 4 and 10 are similar. The solid temperature curves are parallel to the fluid temperature curves along the flow direction. As the Reynolds number decreases, the temperature difference between the solid and fluid phases increases.

EFFECTS OF METAL FOAM PARAMETERS

Equation (25) shows that the volumetric convective heat transfer coefficient is affected by the fiber diameter, d_f, and the cell size, d_p. However, in most cases, only the porosity, ε, and pore density, PPI, of the metal foam are given. The correlations presented by Calmidi [5] were used to estimate the fiber diameter, d_f, and the cell size, d_p:

$$\frac{d_f}{d_p} = 1.18\sqrt{\frac{(1-\varepsilon)}{3\pi}}\left(\frac{1}{1-e^{-(1-\varepsilon)/0.04}}\right), \quad (48)$$

$$d_p = \frac{0.0254}{\mathrm{PPI}} \quad (49)$$

Combining Eqs. (48), (49) and (7), means Eq. (25) can now be expressed as a function of the porosity, ε, pore density, PPI, solid thermal conductivity, k_s, fluid thermal conductivity, k_f, the Reynolds number, Re_d, and the Prandtl number, Pr:

$$h_{sf} = h(\varepsilon, PPI, k_s, k_f, Re_d, Pr) \quad (50)$$

Therefore, the effect of the metal foam parameters (i.e., the porosity, ε, pore density, PPI, and solid thermal conductivity, k_s) can be obtained.

Pore Density

Figure 10 shows the effects of pore density on the volumetric convective heat transfer coefficient. The volumetric convective heat transfer coefficient significantly increases as the pore density increases. This occurs because the cell size decreases as the pore density increases, which causes an increase in the volumetric surface area between the foam ligaments and the fluid. The result is enhanced heat transfer between the solid and fluid phases.

Porosity

Figure 11 shows the effect of porosity on the volumetric convective heat transfer coefficient. The relationship between the volumetric convective heat transfer coefficient and porosity varies as the porosity increases. Figure 11 shows that when the porosity is less than 0.95, the volumetric

convective heat transfer coefficient slightly increases as the porosity increases. However, when the porosity surpasses 0.95, the volumetric convective heat transfer coefficient begins to decrease.

This phenomenon is primarily caused by variations in the foam ligament diameter, d_f. Figure 12 shows that the relationship between the foam ligament diameter and porosity varies in the opposite direction to the relationship between the volumetric convective heat transfer coefficient and the porosity. When the porosity exceeds 0.95, then the foam ligament diameter increases, which increases the heat transfer resistance. As the porosity increases, the percentage of the solid phase (with the higher thermal conductivity) decreases, which then reduces the heat transfer. Thus, the volumetric convective heat transfer coefficient slightly decreases after a critical porosity as the porosity increases. Therefore, only a small amount of metal foam should be used to optimally enhance heat transfer; however, the amount should not be too small.

Solid Thermal Conductivity

Figure 13 shows the volumetric convective heat transfer coefficient for three kinds of metal foam materials: stainless steel, aluminum and copper. All three metal foams have the same porosity (0.9) and pore density (10 PPI). The thermal conductivities of the stainless steel, aluminum and copper were 16.3, 202.4 and 387.6 W/(m·K), respectively.

For each kind of metal foam, the volumetric convective heat transfer coefficient increases as the velocity increases. At low velocities, the solid thermal conductivity has little effect. However, at high velocities, the high solid thermal conductivity significantly increases the volumetric

convective heat transfer coefficient. At the same velocity, the volumetric convective heat transfer coefficients of the aluminum and copper foams are higher than that of the stainless-steel foam with little difference between the volumetric convective heat transfer coefficients of the copper and aluminum foams. Unlike the effect of the pore density, the effect of the solid thermal conductivity on the volumetric convective heat transfer coefficient has an upper limit.

At fixed velocity, there is a critical solid thermal conductivity beyond which the volumetric convective heat transfer coefficient is not significantly influenced by the solid thermal conductivity. Figure 14 shows the effects of the solid thermal conductivity on the volumetric convective heat transfer coefficient at a velocity of 8 m/s. When the thermal conductivity of the metal foam is relatively small, the volumetric convective heat transfer coefficient rapidly increases as the thermal conductivity increases. However, when the thermal conductivity is greater than 150 W/(m·K), then the curve flattens. Therefore, the critical value of the solid thermal conductivity is 150 W/(m·K) at 8 m/s.

CONCLUSIONS

This paper presents an improved model for the volumetric convective heat transfer coefficient in porous foams. The model is based on the convective heat transfer in the pores and the thermal conduction in each foam ligament in the local cubic cell. Numerical results from the present model agree well with experimental data.

The velocity distribution in a metal foam-filled channel is more uniform than in an empty channel with a thinner wall boundary layer. The temperature differences between the fluid and solid phases in sample 10 are quite large, especially for smaller Reynolds numbers. The volumetric convective heat transfer coefficient significantly increases as the pore density increases. However, as the porosity increases, the volumetric convective heat transfer coefficient first increases and then decreases. The volumetric convective heat transfer coefficient significantly increases with large solid thermal conductivities at high velocities. However, there is an upper limit for the effect of the solid thermal conductivity on the volumetric convective heat transfer coefficient. The critical value is approximately 150 W/(m·K) at 8 m/s.

ACKNOWLEDGMENTS

The authors acknowledge financial support for this work from the National Natural Science Foundation of China (No. 51236007).

NOMENCLATURE

A_{cs}	Cross-sectional area of the cylinder, m^2
A_h	Heat transfer area of the cylinder, m^2
a_{sf}	Surface area density, m^{-1}
Bi	Biot number
C_f	Heat capacity of the fluid, J/(kg·K)
d_f	Diameter of the metal foam fibers, m
d_p	Pore size, m

D_h	Hydraulic diameter of the channel, m
F	Inertial coefficient, m^{-1}
H	Channel height, m
h	Convective heat transfer coefficient, $W/(m^2 \cdot K)$
h_{sf}	Interfacial heat transfer coefficient, $W/(m^2 \cdot K)$
k	Thermal conductivity, $W/(m \cdot K)$
K	Permeability, m^2
l	Cylinder
L	Channel length, m
m	$m = \sqrt{\frac{2h}{k_s d_f}}$, m^{-1}
Nu	Averaged Nusselt number
p	Pressure
PPI	Pores per inch
Pr	Prandtl number
Re	Reynolds number
r	Inner-to-outer diameter ratio
u	Local velocity, m/s
q	Heat flux, W/m^2
Q	Heat transfer rate, W
R	Simplification quantity
T	Temperature, K
$\overline{T}$	Average temperature, K
$\vec{v}$	Surperficial velocity

V_1	Cylinder volume, m^3
V_c	Local cell volume, m^3
W	Channel with, m
x	x-coordinate
y	y-coordinate
z	z-coordinate

Greek Symbols

θ	Temperature, $\theta = T_{1c} - T_f$, K
ρ	Density, kg/m^3
ρ_r	Relative density, kg/m^3
μ	Dynamic viscosity, Pa·s
ε	Porosity
Φ	Heat transfer source item

Subscripts

c	Center
d	Dispersion
eff	Effective
s	Solid
se	Solid effective
f	Fluid
fe	Fluid effective
in	Inlet
m	Mean
w	Wall
1,2…6	Tips of the cylinders

Hui Wang is a Ph.D. student at the School of Energy and Power Engineering, Xi'an Jiaotong University, under the supervision of Prof. Liejin Guo. She is currently working on the flow and heat transfer characteristics in metal foam media under numerical, theoretical and experimental aspects.

Liejin Guo is a professor at the School of Energy and Power Engineering, Xi'an Jiaotong University. He received his Ph.D. degree in thermal engineering from Xi'an Jiaotong University in 1989. He is now the director of the State Key Laboratory of Multiphase Flow in Power Engineering. His main research interests include multiphase flow in petroleum engineering, enhanced heat transfer, hydrogen production by biomass gasification in supercritical water and from solar energy, high-pressure steam-water two-phase flow and boiling heat transfer.

REFERENCES

[1] Zhao, C.Y., Review on Thermal Transport in High Porosity Cellular Metal Foams with Open Cells, *International Journal of Heat and Mass Transfer*, vol. 55, no. 13–14, pp. 3618-3632, 2012.

[2] Boomsma, K., Poulikakos, D. and Zwick, F., Metal Foams as Compact High Performance Heat Exchangers, *Mechanics of Materials*, vol. 35, no. 12, pp. 1161-1176, 2003.

[3] Wang, H. and Guo, L., Experimental Investigation on Pressure Drop and Heat Transfer in Metal Foam Filled Tubes under Convective Boundary Condition, *Chemical Engineering Science*, vol. 155, no. 1, pp. 438-448, 2016.

[4] Han, X., Wang, Q., Park, Y., T'Joen, C., Sommers, A. and Jacobi, A., A Review of Metal Foam and Metal Matrix Composites for Heat Exchangers and Heat Sinks, *Heat Transfer Engineering*, vol. 33, no. 12, pp. 991-1009, 2012.

[5] Calmidi, V.V., Transport Phenomena in High Porosity Fibrous Metal Foams, Ph.D. Thesis, University of Colorado, Boulder, Co,1998., 1998.

[6] Kim, S.Y., Kang, B.H. and Kim, J.-H., Forced Convection from Aluminum Foam Materials in an Asymmetrically Heated Channel, *International Journal of Heat and Mass Transfer*, vol. 44, no. 7, pp. 1451-1454, 2001.

[7] Zhao, T.S. and Song, Y.J., Forced Convection in a Porous Medium Heated by a Permeable Wall Perpendicular to Flow Direction: Analyses and Measurements, *International Journal of Heat and Mass Transfer*, vol. 44, no. 5, pp. 1031-1037, 2001.

[8] Mancin, S., Zilio, C., Diani, A. and Rossetto, L., Experimental Air Heat Transfer and Pressure Drop through Copper Foams, *Experimental Thermal and Fluid Science*, vol. 36, no. 0, pp. 224-232, 2012.

[9] Lu, W., Zhao, C.Y. and Tassou, S.A., Thermal Analysis on Metal-Foam Filled Heat Exchangers. Part I: Metal-Foam Filled Pipes, *International Journal of Heat and Mass Transfer*, vol. 49, no. 15–16, pp. 2751-2761, 2006.

[10] Miwa, S. and Revankar, S.T., Hydrodynamic Characterization of Nickel Metal Foam-Effects of Pore Structure and Permeability, *Heat Transfer Engineering*, vol. 33, no. 9, pp. 800-808, 2012.

[11] Noh, J.-S., Lee, K.B. and Lee, C.G., Pressure Loss and Forced Convective Heat Transfer in an Annulus Filled with Aluminum Foam, *International Communications in Heat and Mass Transfer*, vol. 33, no. 4, pp. 434-444, 2006.

[12] Tzeng, S.-C., Spatial Thermal Regulation of Aluminum Foam Heat Sink Using a Sintered Porous Conductive Pipe, *International Journal of Heat and Mass Transfer*, vol. 50, no. 1–2, pp. 117-126, 2007.

[13] Zhao, C.Y., Lu, W. and Tassou, S.A., Thermal Analysis on Metal-Foam Filled Heat Exchangers. Part II: Tube Heat Exchangers, *International Journal of Heat and Mass Transfer*, vol. 49, no. 15–16, pp. 2762-2770, 2006.

[14] Jeng, T. and Tzeng, S., Forced Convection of Metallic Foam Heat Sink under Laminar Slot Jet Confined by Parallel Wall, *Heat Transfer Engineering*, vol. 28, no. 5, pp. 484-495, 2007.

[15] Huang, Z., Nakayama, A., Yang, K., Yang, C. and Liu, W., Enhancing Heat Transfer in the Core Flow by Using Porous Medium Insert in a Tube, *International Journal of Heat and Mass Transfer*, vol. 53, no. 5, pp. 1164-1174, 2010.

[16] Yang, C., Nakayama, A. and Liu, W., Heat Transfer Performance Assessment for Forced Convection in a Tube Partially Filled with a Porous Medium, *International Journal of Thermal Sciences*, vol. 54, no. 0, pp. 98-108, 2012.

[17] Zhao, C., Kim, T., Lu, T. and Hodson, H., Thermal Transport in High Porosity Cellular Metal Foams, *Journal of Thermophysics and Heat Transfer*, vol. 18, no. 3, pp. 309-317, 2004.

[18] Amiri, A. and Vafai, K., Analysis of Dispersion Effects and Non-Thermal Equilibrium, Non-Darcian, Variable Porosity Incompressible Flow through Porous Media, vol. 37, no. 6, pp. 939-954, 1994.

[19] Ichimiya, K., A New Method for Evaluation of Heat Transfer between Solid Material and Fluid in a Porous Medium, *Journal of Heat Transfer*, vol. 121, no. 4, pp. 978-983, 1999.

[20] Golombok, M., Jariwala, H. and Shirvill, L.C., Gas-Solid Heat Exchange in a Fibrous Metallic Material Measured by a Heat Regenerator Technique, *International Journal of Heat and Mass Transfer*, vol. 33, no. 2, pp. 243-252, 1990.

[21] Younis, L. and Viskanta, R., Experimental Determination of the Volumetric Heat Transfer Coefficient between Stream of Air and Ceramic Foam, *International Journal of Heat and Mass Transfer*, vol. 36, no. 6, pp. 1425-1434, 1993.

[22] Hwang, J.-J., Hwang, G.-J., Yeh, R.-H. and Chao, C.-H., Measurement of Interstitial Convective Heat Transfer and Frictional Drag for Flow across Metal Foams, *Journal of Heat Transfer*, vol. 124, no. 1, pp. 120-129, 2002.

[23] Giani, L., Groppi, G. and Tronconi, E., Heat Transfer Characterization of Metallic Foams, *Industrial & engineering chemistry research*, vol. 44, no. 24, pp. 9078-9085, 2005.

[24] Jiang, P.-X., Xu, R.-N. and Gong, W., Particle-to-Fluid Heat Transfer Coefficients in Miniporous Media, *Chemical Engineering Science*, vol. 61, no. 22, pp. 7213-7222, 2006.

[25] Lu, T., Stone, H. and Ashby, M., Heat Transfer in Open-Cell Metal Foams, *Acta Materialia*, vol. 46, no. 10, pp. 3619-3635, 1998.

[26] Zhao, C., Kim, T., Lu, T. and Hodson, H., Thermal Transport Phenomena in Porvair Metal Foams and Sintered Beds, University of Cambridge Engineering Department Report, Cambridge, UK, August, 2001.

[27] Boomsma, K., Poulikakos, D. and Ventikos, Y., Simulations of Flow through Open Cell Metal Foams Using an Idealized Periodic Cell Structure, *International Journal of Heat and fluid flow*, vol. 24, no. 6, pp. 825-834, 2003.

[28] Kwon, Y.W., Cooke, R.E. and Park, C., Representative Unit-Cell Models for Open-Cell Metal Foams with or without Elastic Filler, *Materials Science and Engineering: A*, vol. 343, no. 1–2, pp. 63-70, 2003.

[29] Krishnan, S., Garimella, S.V. and Murthy, J.Y., Simulation of Thermal Transport in Open-Cell Metal Foams: Effect of Periodic Unit-Cell Structure, *Journal of Heat Transfer*, vol. 130, no. 2, pp. 024503-024503, 2008.

[30] Zukauskas, A., Convective Heat Transfer in Cross Flow, Wiley, New York, 1987.

[31] Hsu, C. and Cheng, P., Thermal Dispersion in a Porous Medium, *International Journal of Heat and Mass Transfer*, vol. 33, no. 8, pp. 1587-1597, 1990.

[32] Vafai, K. and Tien, C., Boundary and Inertia Effects on Flow and Heat Transfer in Porous Media, *International Journal of Heat and Mass Transfer*, vol. 24, no. 2, pp. 195-203, 1981.

[33] Boomsma, K. and Poulikakos, D., On the Effective Thermal Conductivity of a Three-Dimensionally Structured Fluid-Saturated Metal Foam, *International Journal of Heat and Mass Transfer*, vol. 44, no. 4, pp. 827-836, 2001.

[34] Amiri, A., Vafai, K. and Kuzay, T., Effects of Boundary Conditions on Non-Darcian Heat Transfer through Porous Media and Experimental Comparisons, *Numerical Heat Transfer, Part A: Applications*, vol. 27, no. 6, pp. 651-664, 1995.

[35] Alazmi, B. and Vafai, K., Constant Wall Heat Flux Boundary Conditions in Porous Media under Local Thermal Non-Equilibrium Conditions, *International Journal of Heat and Mass Transfer*, vol. 45, no. 15, pp. 3071-3087, 2002.

[36] Lee, D.-Y. and Vafai, K., Analytical Characterization and Conceptual Assessment of Solid and Fluid Temperature Differentials in Porous Media, *International Journal of Heat and Mass Transfer*, vol. 42, no. 3, pp. 423-435, 1999.

Table 1. Structural parameters of the foam samples in Zhao et al. [26]

Sample number	Materials	Pore size PPI	Relative density (ρ_r)	Inner-to-outer diameter ratio (r)	Fiber diameter d_f (μm)	Cell size d_p (mm)
Sample 4	FeCrAlY	30	0.102	0.4	267	2.089
Sample 10	Copper	10	0.082	-	270	2.697

List of Figure Captions

Figure 13. Interfacial convective heat transfer coefficient plotted as a function of velocity

Figure 14. Effect of the solid thermal conductivity on the volumetric convective heat transfer coefficient

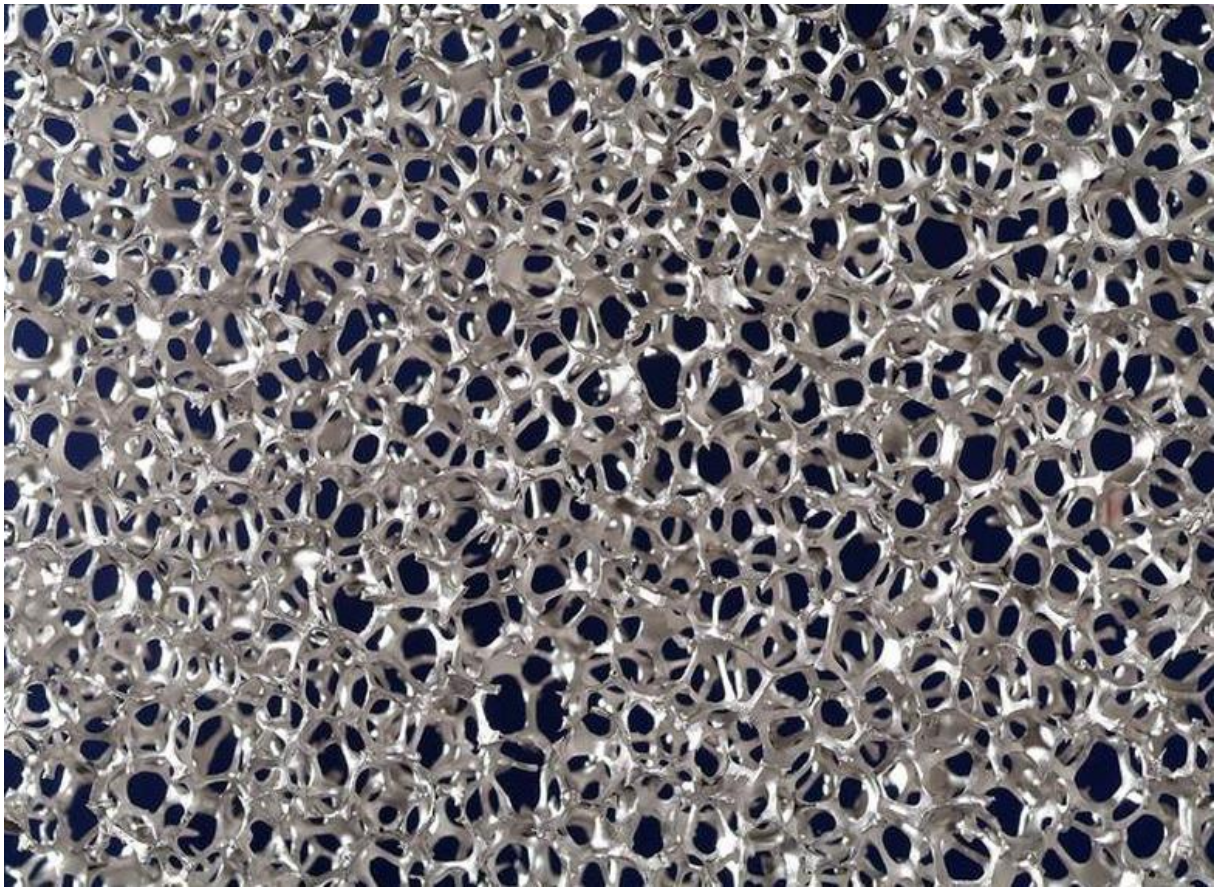

Figure 1. Typical metal foam structure

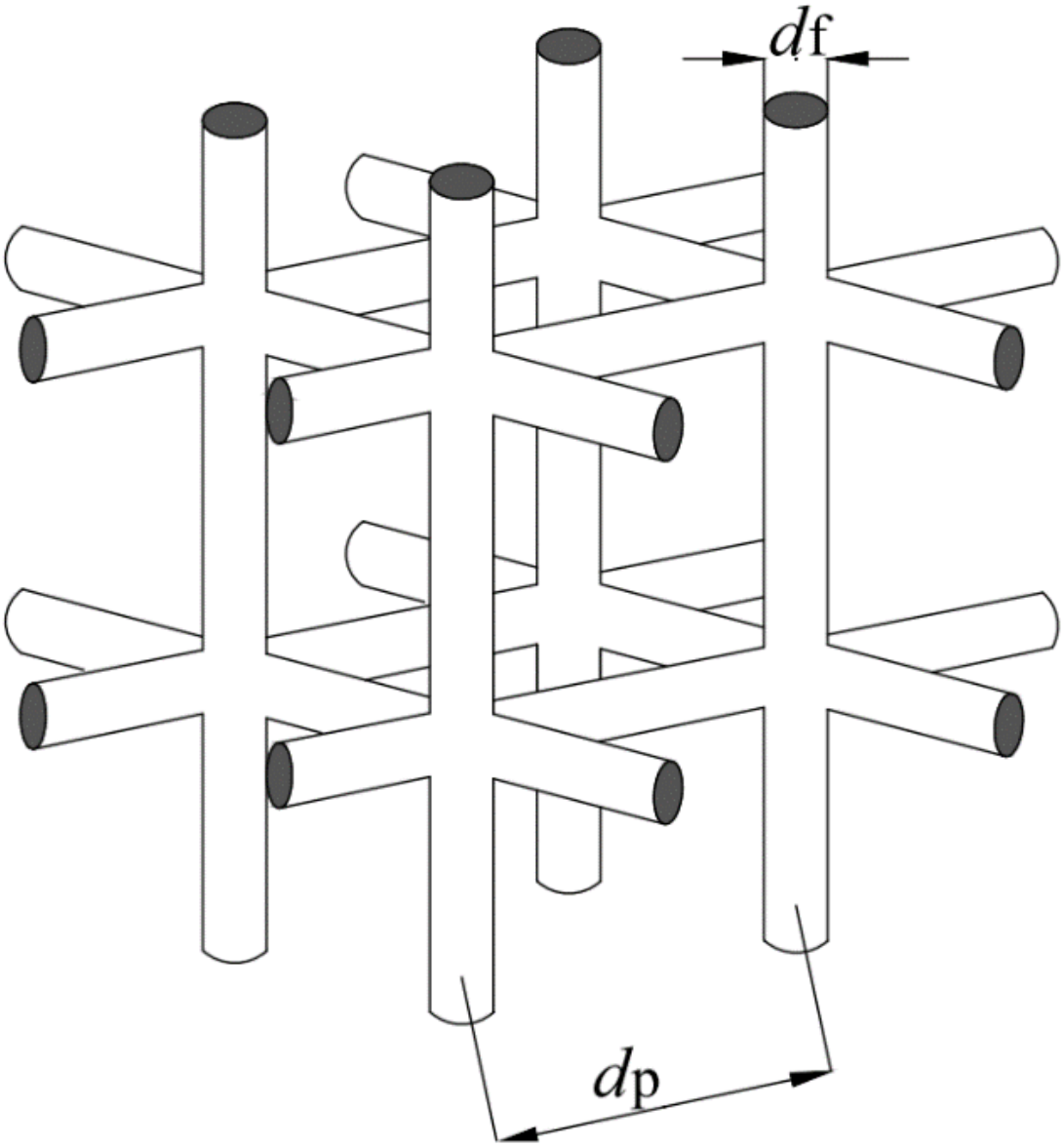

Figure 2. Open-cell representation of a metal foam structure

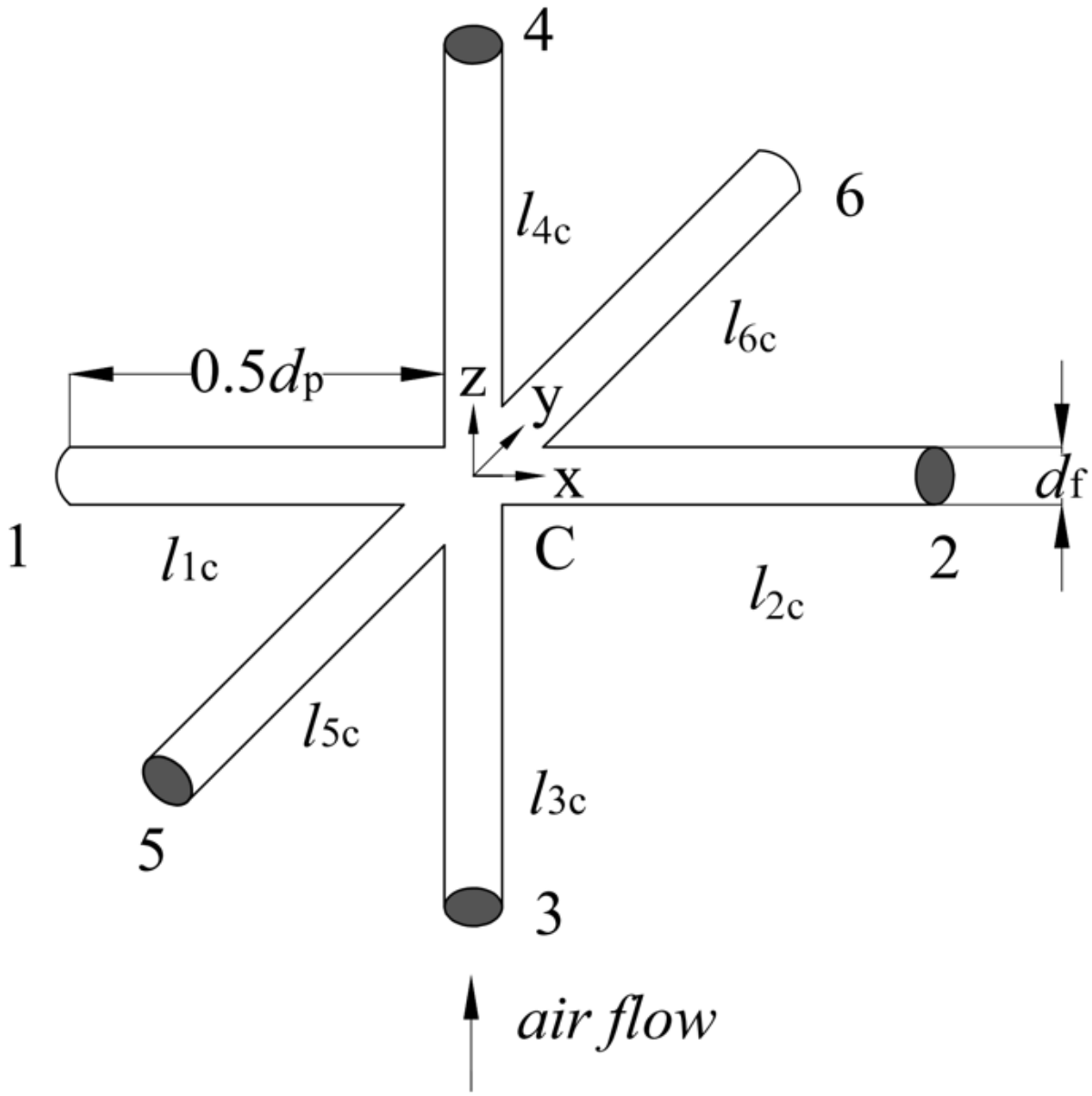

Figure 3. Local cell of a metal foam

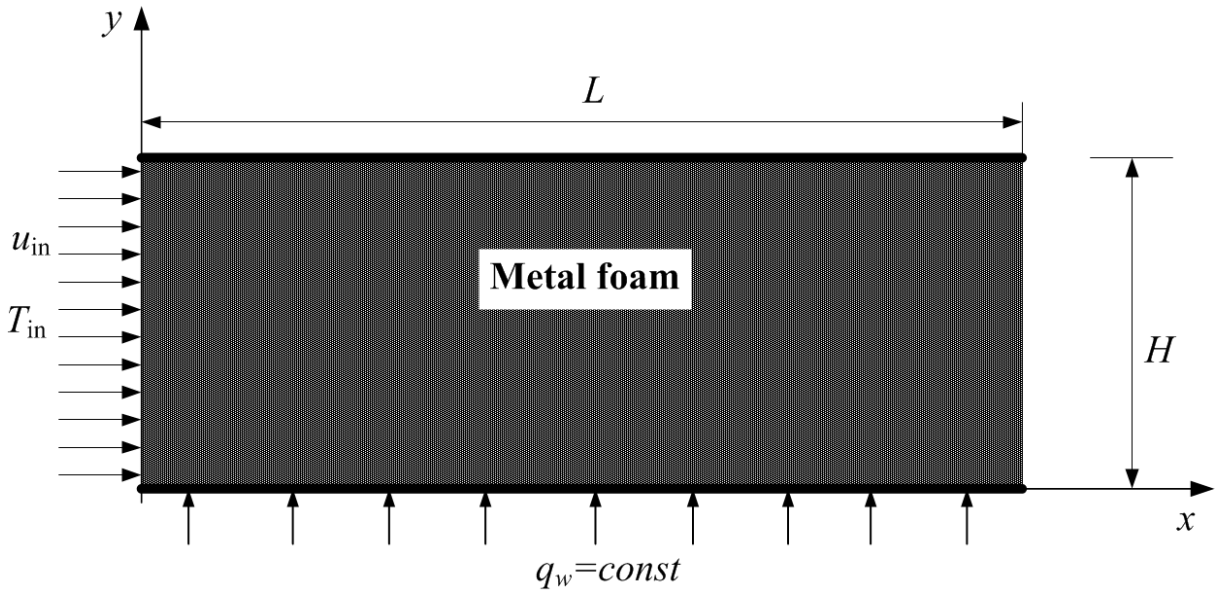

Figure 4. Schematic diagram of a metal foam-filled channel

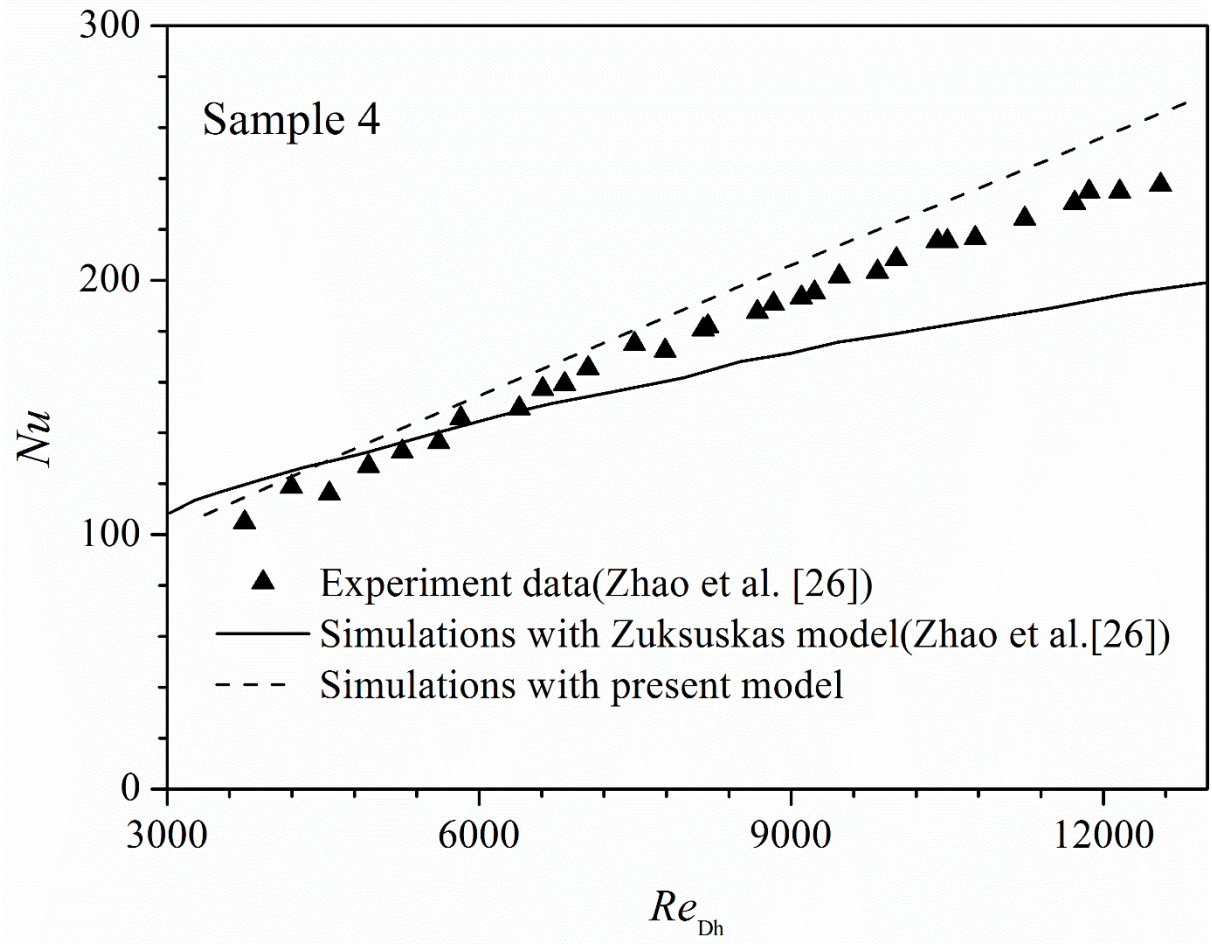

Figure 5. Comparison of the average Nusselt numbers for sample 4

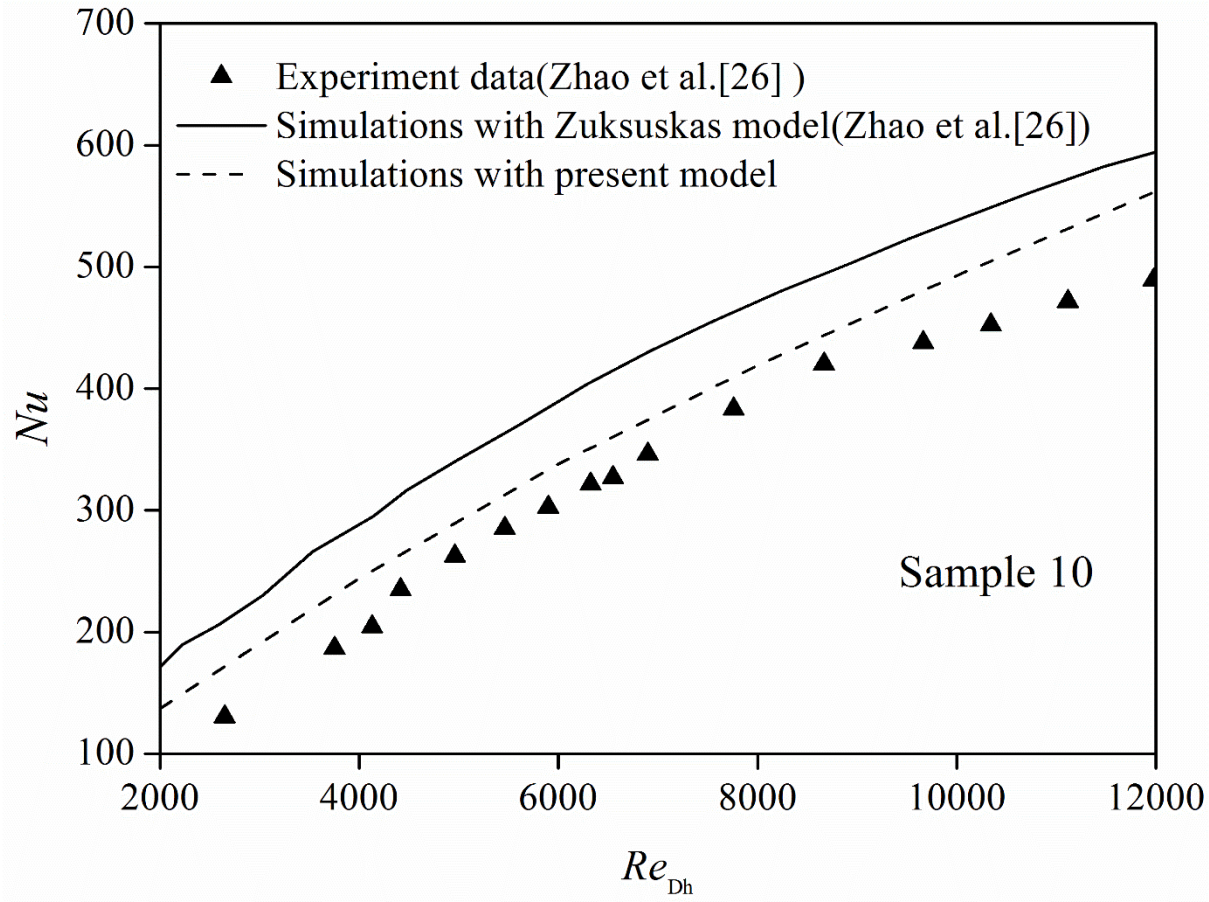

Figure 6. Comparisons of average Nusselt numbers for sample 10

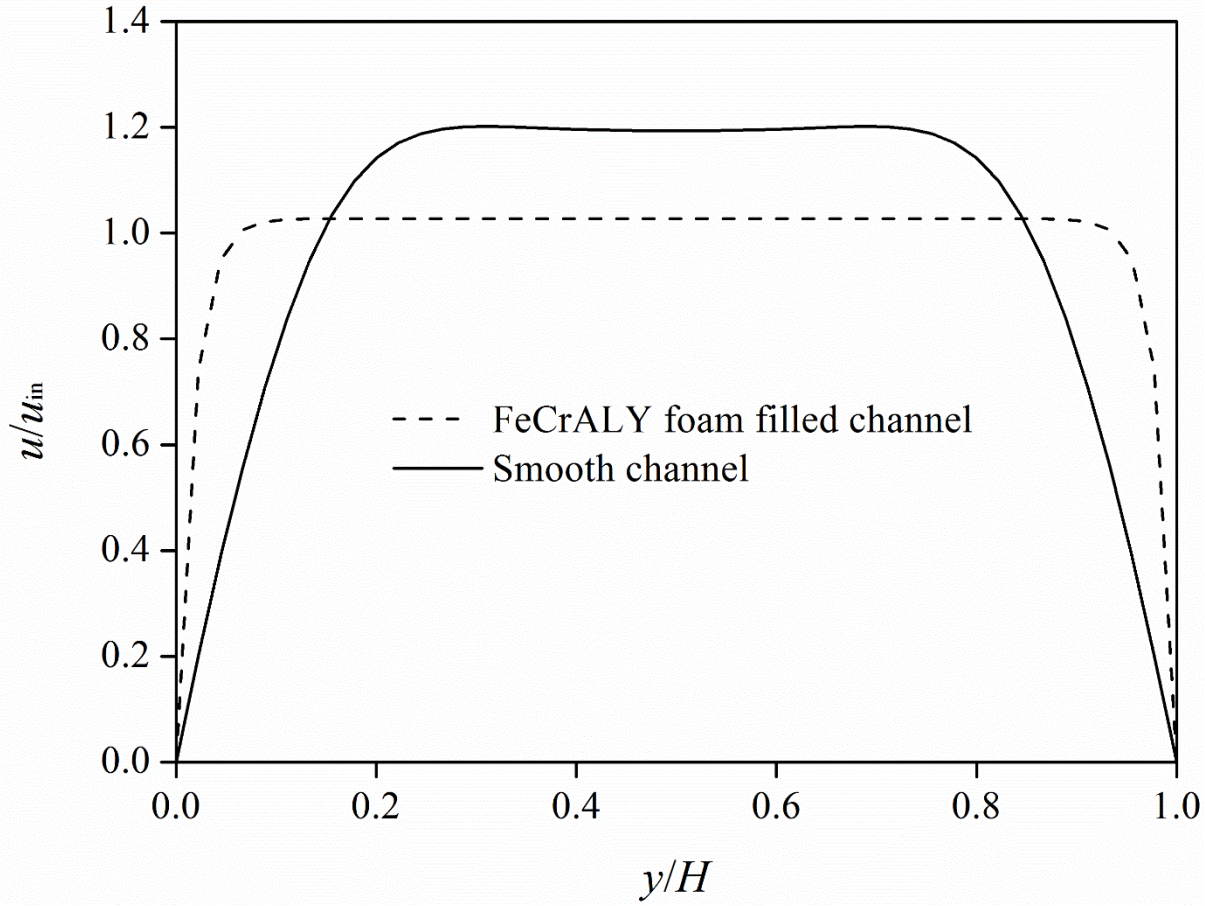

Figure 7. Comparison of the velocity distributions in metal foam-filled and empty channels

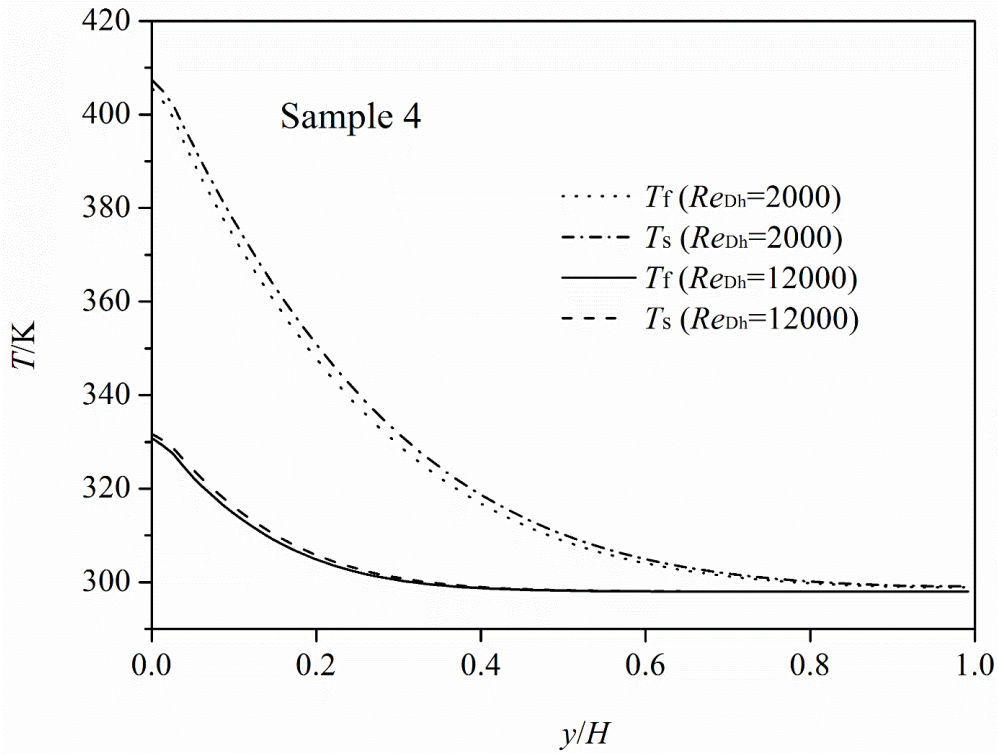

(a) Sample 4

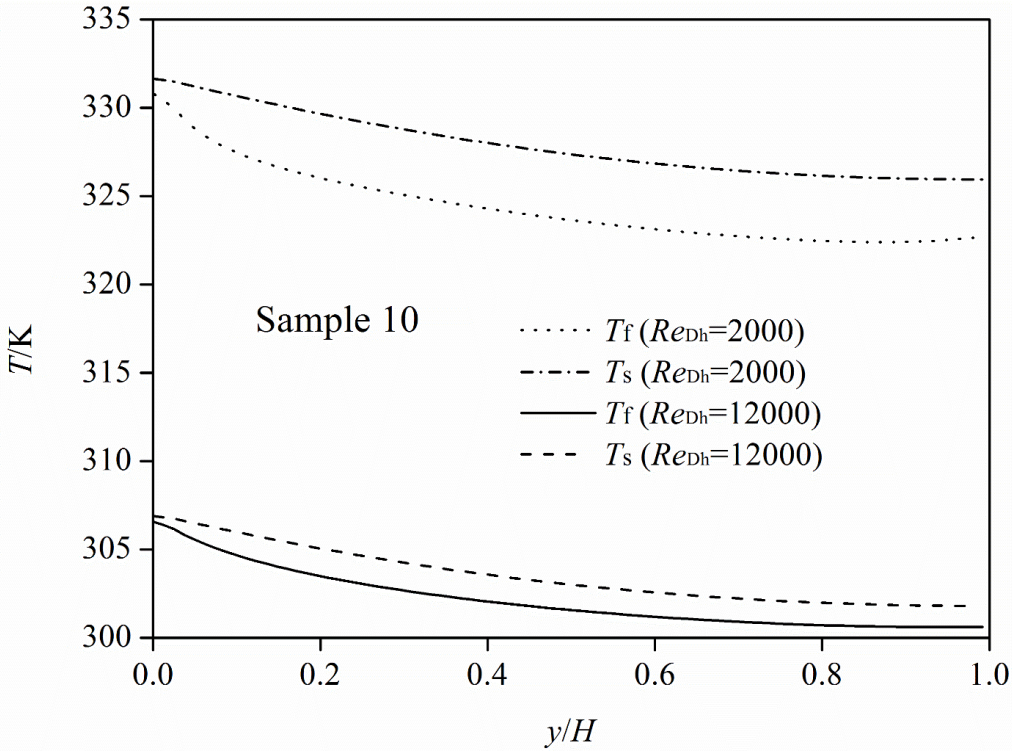

(b) Sample 10

Figure 8. Solid and fluid temperature distributions along the vertical direction at *x*/*H*=5

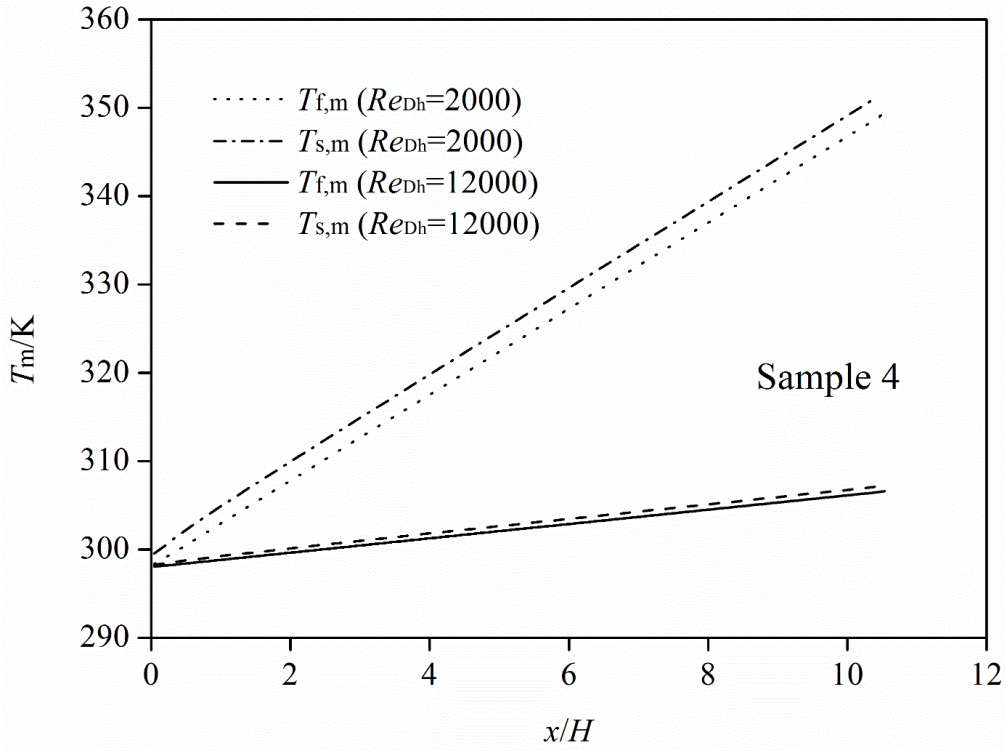

(a) Sample 4

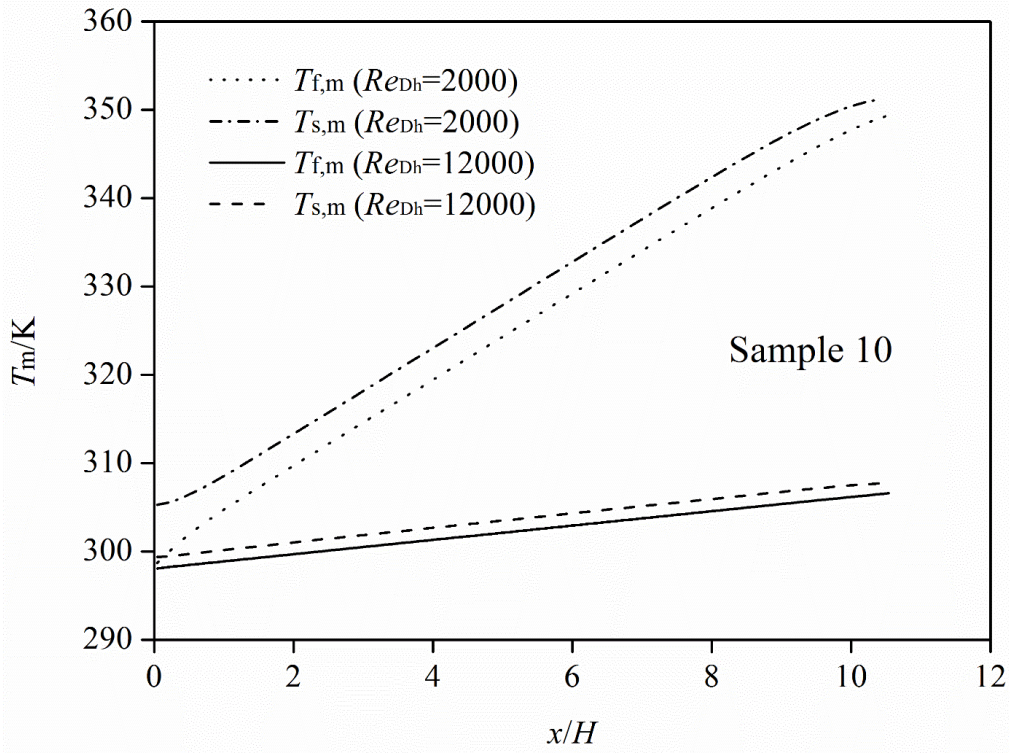

(b) Sample 10

Figure 9. Average solid and fluid temperature distributions along the flow direction

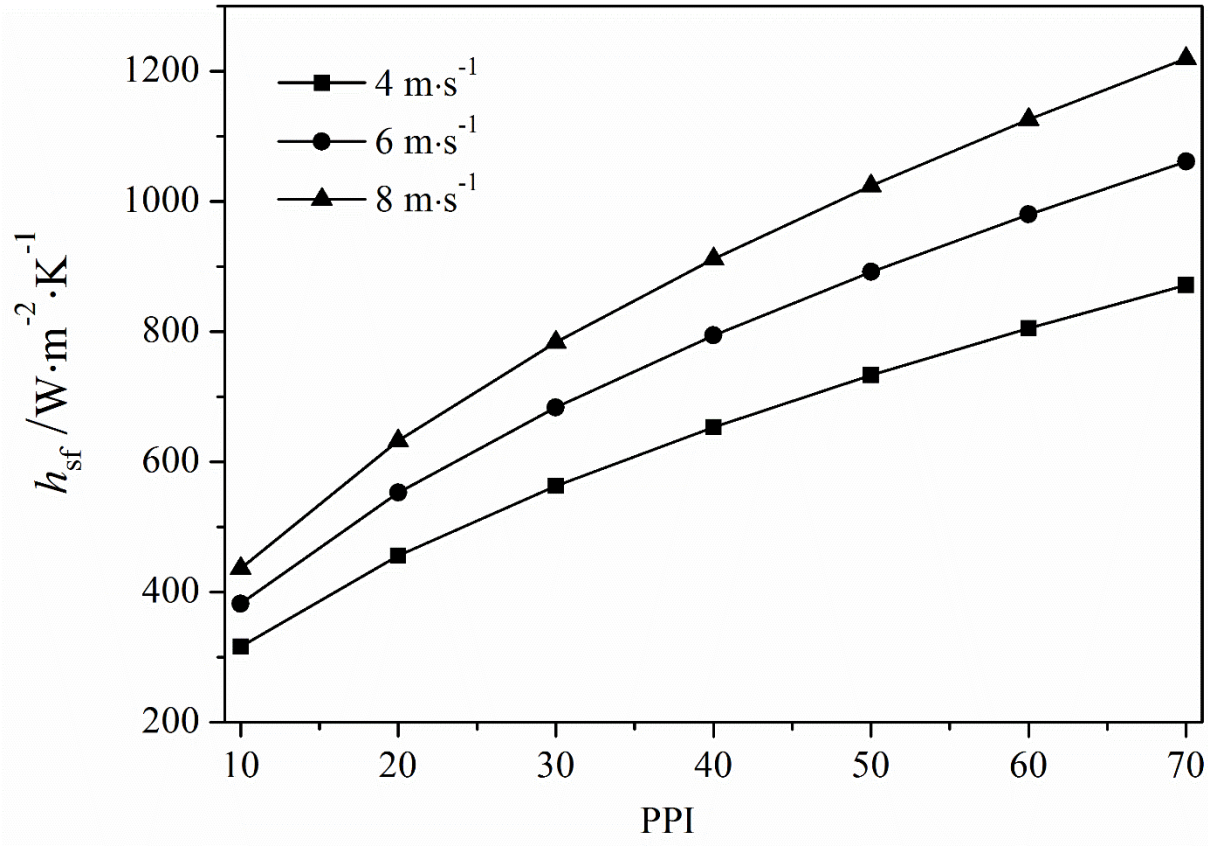

Figure 10. Effect of pore density on the volumetric convective heat transfer coefficient (ε=0.93)

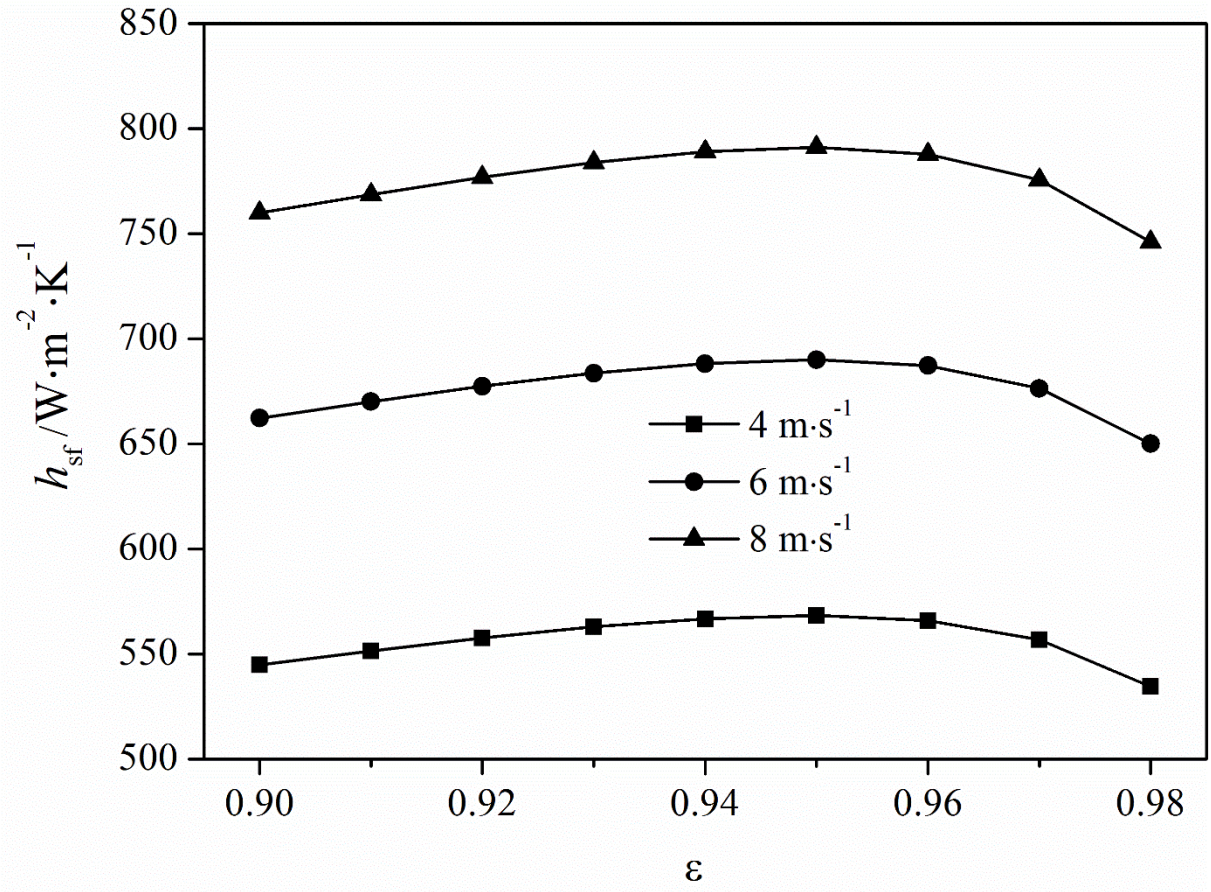

Figure 11. Effect of porosity on the volumetric convective heat transfer coefficient (PPI=30)

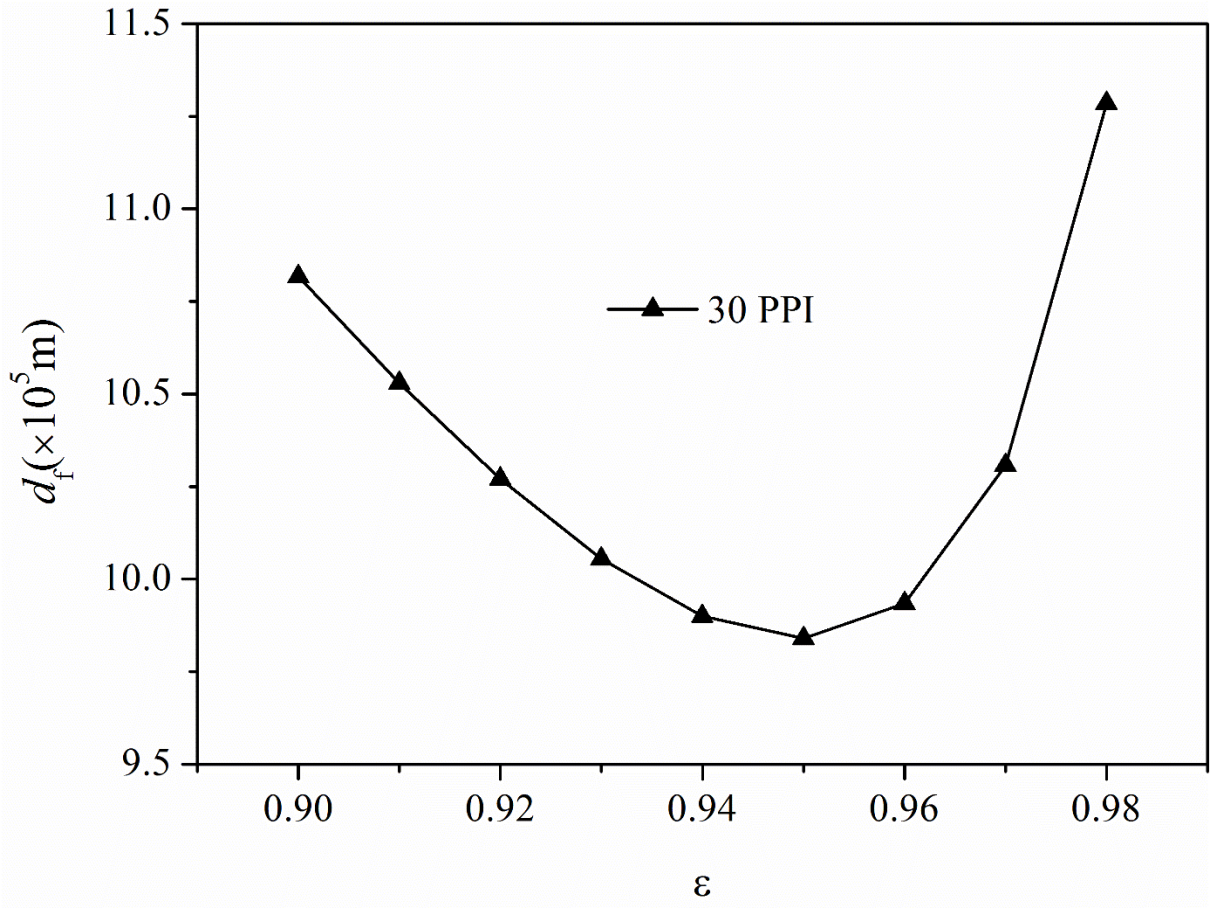

Figure 12. Effect of the porosity on the foam ligament diameter

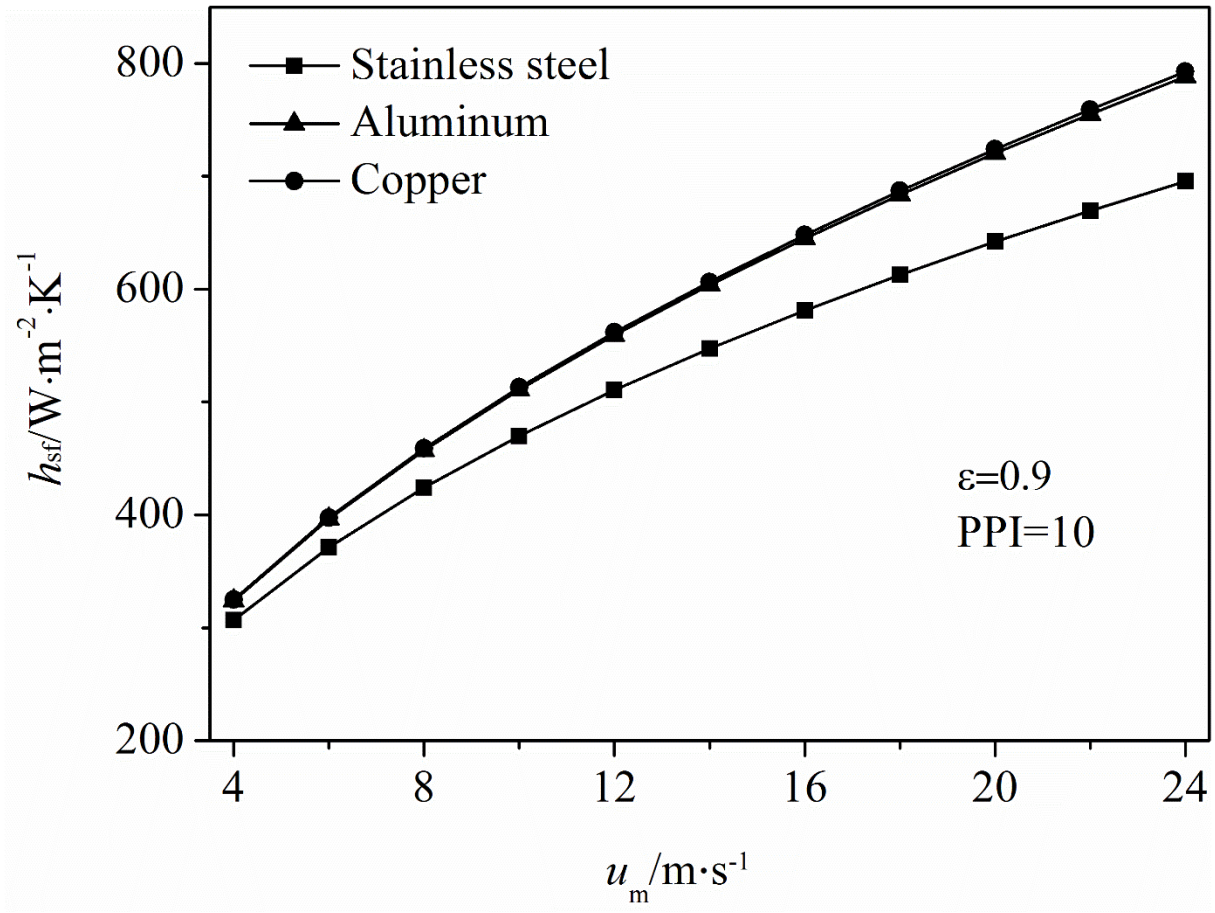

Figure 13. Interfacial convective heat transfer coefficient plotted as a function of velocity

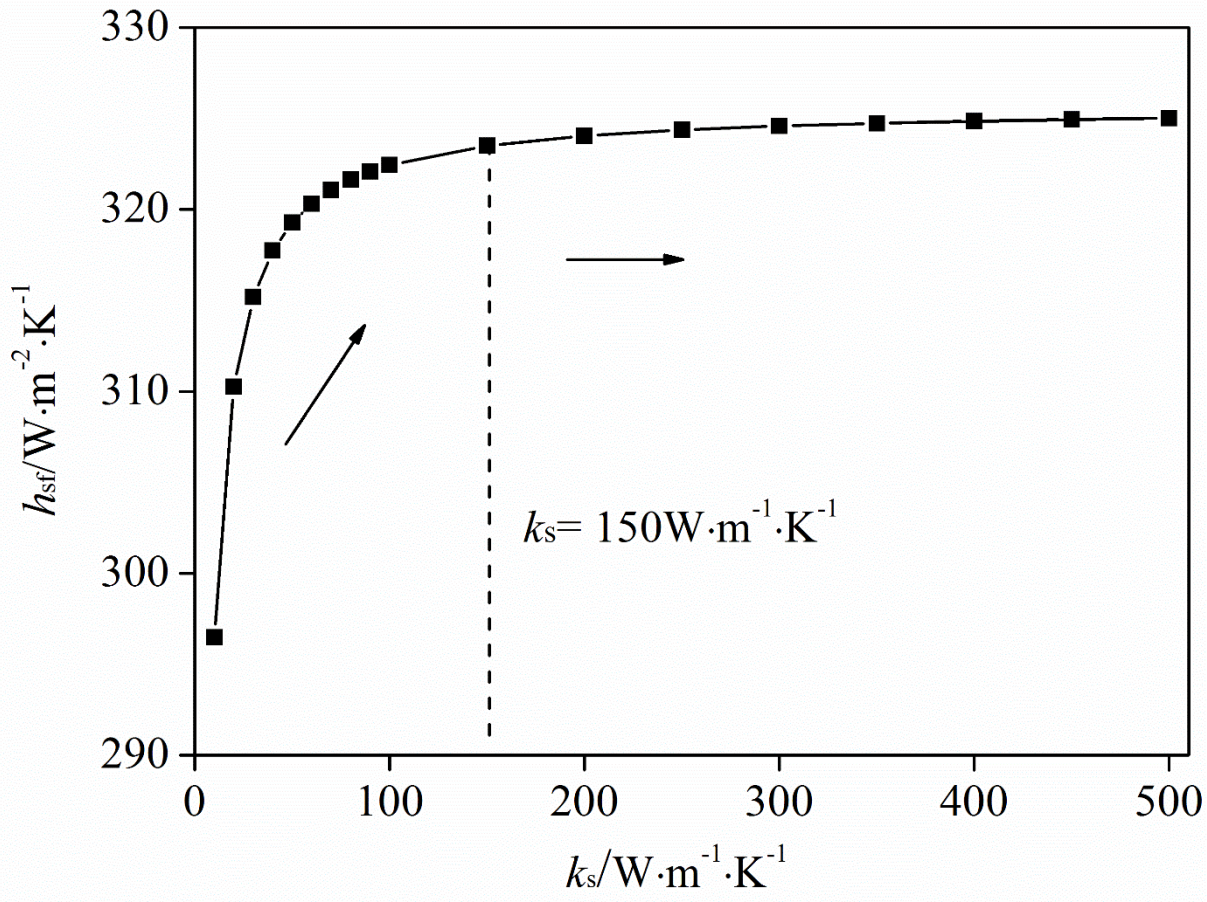

Figure 14. Effect of the solid thermal conductivity on the volumetric convective heat transfer coefficient